Trajectory Planning of a Weather Balloon with Altitude Control Subject to Wind Disturbances

Ana Catarina Rita Rodrigues
a.catarina.rodrigues@tecnico.ulisboa.pt

Instituto Superior Técnico, Lisboa, Portugal

June 2023

Abstract

Weather balloons are widely used to collect atmospheric data above the ground and to perform atmospheric research, due to their low-cost and simplicity. However, their flight is dependent of the atmospheric conditions and their life cycle is short. Thus, altitude and trajectory control of weather balloons is a major area of interest, as it would allow a more accurate exploration of the atmosphere. Since the existing control solutions are dependent of wind currents, path planning is a crucial step to be able to direct the balloon to desired areas. This work focuses on the development of a path planning algorithm as well as a realistic simulator, with an existing altitude control strategy. The work is divided in three main parts: 1) development of a balloon model and simulator, 2) wind statistical analysis, and 3) development of a balloon path planning solution. In the first part, a realistic balloon model is derived, and a simulator is implemented, with wind disturbances and an altitude controller. The second part focuses on the feasibility of using wind currents to direct the balloon, performing a thorough statistical analysis of the wind behavior. Finally, the third part focuses on the development of a balloon path planning solution and validation with different scenarios and mission objectives. The objectives defined for this thesis were achieved, and it was demonstrated that it is possible to direct a weather balloon to desired areas with an altitude control strategy and taking advantage of wind currents.
Keywords: Weather balloon, Balloon modeling, Wind analysis, Path planning, A* algorithm

1. Introduction

Weather balloons are a type of high altitude balloons specifically used to carry research payloads into the upper atmosphere and are considered to be the primary source to retrieve atmospheric data above the ground. Twice a day, every day of the year, weather balloons are released simultaneously from almost 900 locations across the world, providing a ”snapshot” of the Earth’s atmosphere. They retrieve data, such as temperature, humidity and wind currents, among many others, which are valuable for forecast models and meteorologists.

Apart from being an indispensable tool in meteorology and other applications requiring stratospheric observations, weather balloons have also proven to be a suitable alternative for atmospheric research. They appear as a low-cost alternative to satellites and aircrafts, which are expensive to build and maintain, and they require far less power than its alternatives since they fly due to buoyancy.

However, weather balloons are dependent on atmospheric conditions, making it challenging to accurately estimate their trajectory and duration of flight. This is undesirable since the data they collect might not always be what is needed. This constraint combined with their short life cycle makes altitude and trajectory control for weather balloons a key area of interest. It would allow to direct the balloon to desired areas, extend the flight’s duration and perform a more precise research of the atmosphere while maintaining the advantages of using them for scientific research.

The Synchronous Oceanic and Atmospheric Data Acquisition (SONDA) project appears in this context, with the objective to better monitor the atmosphere and ocean by proposing the development of an innovative system, complementary to the existing means of observation. In the scope of the SONDA project, this work aims to provide some positioning capability to the balloon system, by controlling its altitude in agreement with the available wind currents.

1.1. State-of-the-Art in Balloon Planning and Control

There are various state-of-the-art altitude control solutions which aim to maintain balloons at desired altitudes so that they do not rise indefinitely, to allow atmospheric observation and research as well as weather monitoring and communications, and to

extend the flights duration [1, 2, 3, 4].

In addition to altitude control, trajectory control may also be necessary to guide the balloon to desired locations, avoid prohibited areas, among others. According to the state-of-the-art solutions, to control a balloon's trajectory it is necessary to either combine an altitude control mechanism with wind changes [5, 6], or to physically alter the balloon and take advantage of the wind [7].

Since the majority of control strategies depend of the wind's behavior, path planning is a crucial step to optimize the balloon trajectory and ensure the balloon reaches the desired location. Balloon path planning is a field that has not been extensively researched, but some approaches have been explored, such as using graph-based path planning [8, 9], stochastic solutions [10, 11] and bio-inspired algorithms [12, 13].

According to the literature review, almost no solutions have been developed for latex balloons. Since weather balloons are inexpensive, being able to properly adapt the established control techniques to manage latex balloons and implement an optimization algorithm to find an optimal path from start to goal locations would be a good, affordable solution that would enable a more accurate and extensive exploration of the atmosphere.

2. Balloon Model and Simulator

The balloon structure is not only composed by the balloon's envelope but also by an attached payload, which may comprise a variety of equipment. For this work, the balloon's model was defined considering that the payload was composed, among others, by a valve and an hopper, which are the required equipment to implement the altitude control developed by B.Cândido [14]. This altitude control is achieved by mass variation, where the balloon descends when gas is released and ascends when ballast is released.

Furthermore, in order to obtain the balloon model, this was sub-divided in 4 parts: atmospheric, geometric, thermal and dynamics model.

2.1. Atmospheric Model

The balloon system requires an atmospheric model to properly account the impact of the atmosphere on the balloon dynamics. Hence, the International Standard Atmosphere (ISA) model will be use, which provides, among others, values for temperature T_{atm}, pressure P_{atm} and density ρ_{atm} based on the altitude z [m]. Figure 1 shows the correlation between atmospheric temperature, pressure and density with altitude.

2.2. Geometric Model

For accurate modeling of forces and heat loads acting on the balloon, understanding of the geometric

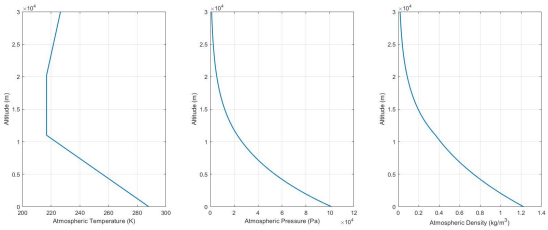

Figure 1: International Standard Atmosphere model.

parameters of the balloon is required. The properties of a latex balloon can be derived by the following equations, assuming the balloon is approximated to a sphere:
Projected area [m^2]:

$$A_p = \pi R^2 \,, \tag{1}$$

Surface area [m^2]:

$$A_s = 4A_p \,, \tag{2}$$

Volume [m^3]:

$$V_b = \frac{4}{3}\pi R^3 \,, \tag{3}$$

Membrane thickness [m]:

$$t = \frac{V_b}{A_s} = \frac{m_b}{4\pi R^2 \cdot \rho_b} \,, \tag{4}$$

where m_b is the balloon envelope mass, ρ_b is the balloon envelope density and R is the balloon radius.

A latex balloon has always more pressure inside than outside its envelope because rubber applies a restoring force inwards. This relation is depicted as

$$P_{in} = \Delta P + P_{out} \,, \tag{5}$$

where P_{in} is the pressure inside the balloon, ΔP is the membrane pressure and P_{out} is the atmospheric pressure (P_{atm}).

Since a latex balloon deforms in a non-linear way, the balloon radius should be obtain through a hyper-elastic theory instead of the perfect gas law to obtain a more accurate model. The Mooney-Rivlin model is described by:

$$\Delta P = 2s_+ \frac{t_0}{R_0}\left(\left(\frac{R_0}{R}\right) - \left(\frac{R_0}{R}\right)^7\right)\left(1 - \frac{s_-}{s_+}\left(\frac{R}{R_0}\right)^2\right) \,, \tag{6}$$

where s_+ (3bar) and s_- (-0.3bar) are constant elastic coefficients, t_0 is the membrane thickness of the uninflated balloon and R_0 is the uninflated balloon radius.

The pressure inside the balloon (P_{in}) can be computed through the perfect gas law

$$\begin{cases} P_g V_b = n R_g T_g \\ n = \frac{m_g}{M_g} \end{cases} \Rightarrow P_g = \frac{m_g R_g T_g}{M_g V_b} \,, \tag{7}$$

where P_g is the pressure of gas inside the balloon, n is the number of moles, R_g is the universal gas constant (8.3144621J/(K $\cdot$ mol)), T_g is the temperature of gas, m_g is the mass of gas inside the balloon and M_g is the molar mass of the gas.

2.3. Thermal Model

During its flight the balloon is subject to various heat loads, specially direct solar radiation and infrared radiation from the Earth, which are absorbed by the balloon's envelope (film). Consequently, the envelope heats the gas inside the balloon by convection and self-glow, and, as a result, the gas inside the balloon expands, the balloon's radius increases, and the buoyancy rises.

2.3.1. Direct Solar Radiation

The direct solar radiation is the electromagnetic radiation emitted by the sun that reaches the Earth's surface without being diffused. The total absorbed direct sun radiation is computed by the following expression:

$$Q_{Sun} = \alpha \cdot A_p \cdot q_{sun} \cdot \left(1 + \frac{\tau}{1-r}\right), \quad (8)$$

where q_{sun} is the direct solar flux, and α, τ and r are optical surface properties (film properties), more specifically α is the solar absorptivity coefficient, τ is the transmissivity coefficient and r is the reflectivity coefficient given by $r = 1 - \alpha - \tau$.

2.3.2. Infrared Radiation

The radiation emitted from Earth is called long-wave radiation and falls within the infrared portion of the electromagnetic spectrum. The total absorbed planetary long-wave heat is obtained by:

$$Q_{IR_{earth}} = \alpha_{IR} \cdot A_s \cdot q_{IR_{earth}} \cdot VF \cdot \left(1 + \frac{\tau_{IR}}{1-r_{IR}}\right), \quad (9)$$

where $q_{IR_{earth}}$ is the long-wave radiation flux from the ground at altitude z, VF is the view factor, and α_{IR} (absorptivity), τ_{IR} (transmissivity) and r_{IR} (reflectivity) are the optical surface properties in the infrared spectrum, with $r_{IR} = 1 - \alpha_{IR} - \tau_{IR}$.

2.3.3. Albedo

The albedo is the fraction of the total incident solar energy that is reflected by a body or surface, in this case the Earth. The total absorved albedo heat is computed by the following expression:

$$Q_{Albedo} = \alpha \cdot A_s \cdot q_{Albedo} \cdot VF \cdot \left(1 + \frac{\tau}{1-r}\right), \quad (10)$$

where q_{Albedo} is the albedo flux.

2.3.4. Film Emissions

The emitted energy from both the interior and exterior of the balloon film, is defined by

$$Q_{IR_{out}} = \sigma \cdot \epsilon \cdot A_s \cdot T_f^4 \cdot \left(1 + \frac{\tau_{IR}}{1-r_{IR}}\right), \quad (11)$$

where T_f is the film temperature and ϵ is the emissivity of the film, which according to the Kirchhoff's law is assumed to be equal to the longwave absorptivity coefficient α_{IR} ($\epsilon = \alpha_{IR}$).

2.3.5. Self-Glow

The absorbed infrared self-glow from the interior of the balloon film accounts for the trapping of the heat due to the multiple internal reflections which affects the film temperature and is computed as follows

$$Q_{IR_{film}} = \sigma \cdot \epsilon \cdot \alpha_{IR} \cdot A_s \cdot T_f^4 \cdot \left(\frac{1}{1-r_{IR}}\right). \quad (12)$$

2.3.6. Convection

Convection is a heat transfer mechanism that, for this system, is divided into internal (transfer between the lifting gas and the balloon's skin) and external convection (transfer between the atmosphere and the balloon skin):

$$Q_{ConvInt} = Hi \cdot A_s \cdot (T_f - T_g), \quad (13)$$

$$Q_{ConvExt} = He \cdot A_s \cdot (T_{atm} - T_f), \quad (14)$$

where Hi and He are the internal and external convection heat transfer coefficients, respectively.

2.3.7. Thermal Balance

Having defined all the considered heat loads acting on the balloon it is now possible to compute the rate of change of temperature (differential equation) of both the gas

$$\dot{T_g} = \frac{Q_{ConvInt}}{c_v \cdot m_g} + (\gamma - 1) \cdot T_g \cdot \left(\frac{dm_g}{dt} \cdot \frac{1}{m_g} - \frac{dV_b}{dt} \cdot \frac{1}{V_b}\right) \quad (15)$$

and the balloon film

$$\dot{T_f} = \frac{Q_{Sun} + Q_{IR_{Earth}} + Q_{Albedo} + Q_{IR_{film}}}{c_f \cdot m_b} + \frac{+Q_{ConvExt} - Q_{IR_{out}} - Q_{ConvInt}}{c_f \cdot m_b}, \quad (16)$$

where c_v is the specific heat at constant volume of the gas, γ is adiabatic expansion coefficient of the gas and c_f is the specific heat of the film.

2.4. Dynamics Model

The forces acting on the balloon system must be identified in order to obtain the differential equations that characterize the balloon dynamics. The main forces acting on the balloon system are buoyancy, gravity (weight), aerodynamic drag and wind.

To simplify the model, the 3D movement of the balloon is decoupled into its vertical and horizontal components, so that they are computed separately.

2.4.1. Vertical Motion

Buoyancy is the force that comes from the Archimedes' Principle and is defined by

$$B = \rho_{atm} \cdot V_b \cdot g \,. \tag{17}$$

Weight represents the force of gravity which pulls the balloon to the center of the Earth as presented

$$W = -m_T \cdot g \,, \tag{18}$$

where m_T is the total mass of the system.

Drag is the force acting opposite to the relative movement of the balloon with respect to the surrounding fluid, in this case, air. Since buoyancy and weight only have a vertical component, the drag force will also only have a component in the vertical direction. This force is computed as shown

$$D = -\frac{1}{2} \cdot C_D \cdot A_p \cdot \rho_{atm} \cdot \dot{z} \cdot |\dot{z}| \,, \tag{19}$$

where C_D is the drag coefficient, which depends on the Reynolds number and on the balloon shape.

Once the forces acting on the system have been identified it is possible to define the differential equation governing the vertical motion of the balloon through a balance of forces

$$\begin{aligned} \sum F = m \cdot a \Leftrightarrow B + W + D = m \cdot \ddot{z} \\ \Leftrightarrow \ddot{z} = \frac{B + W + D}{m_T + m_v} \,, \end{aligned} \tag{20}$$

where $\ddot{z}$ is the vertical acceleration of the balloon and m_v is the virtual mass.

2.4.2. Horizontal Motion

The horizontal movement of the balloon depends on the horizontal wind the balloon is subject to. In this work it is assumed that there is no horizontal slip between the balloon and the surrounding air mass, so the balloon's horizontal velocity is equal to that of the incident wind itself. The wind velocity is composed of two components: longitudinal v_{wx} (x-component) and latitudinal v_{wy} (y-component), which are retrieved from the ERA5 (European Environment Agency) wind database.

The variation of latitude ($\frac{\delta\phi}{\delta t}$) and longitude ($\frac{\delta\lambda}{\delta t}$) are obtained based on the wind velocity components according to the following conversions:

$$\frac{\delta\phi}{\delta t} = \frac{180}{\pi} \frac{v_{wy}}{R_{Earth} + z} \,, \tag{21}$$

$$\frac{\delta\lambda}{\delta t} = \frac{180}{\pi} \frac{v_{wx}}{(R_{Earth} + z) \cdot \cos(\phi \frac{\pi}{180})} \,, \tag{22}$$

where ϕ is the current latitude value expressed in degrees [°].

2.5. Balloon Simulator

The parameters required to validate the balloon model are presented in Tables 1, 2 and 3. Note that for this work the balloon model is the TA450 model, the ballast is sand, and the gas is helium.

Table 1: Balloon parameters.

Parameter	Symbol	Value	Units
Balloon mass	m_b	0.450	kg
Uninflated radius	R_0	0.43	m
Burst radius	R_b	2.36	m
Material mass	$m_{material}$	0.640	kg
Ballast mass	$m_{ballast}$	0.950	kg
Latex (rubber) density	ρ_b	1100	kg/m^3

Table 2: Optical film properties.

Parameter	Symbol	Value	Units
in the solar spectrum			
Solar absorptivity coefficient	α	0.001	-
Transmissivity coefficient	τ	0.885	-
Reflection coefficient	$r = 1 - \alpha - \tau$	0.1140	-
in the infrared spectrum			
Solar absorptivity coefficient	α_{IR}	0.031	-
Transmissivity coefficient	τ_{IR}	0.842	-
Reflection coefficient	$r_{IR} = 1 - \alpha_{IR} - \tau_{IR}$	0.1270	-

Table 3: Gas (Helium) parameters.

Parameter	Symbol	Value	Units
Molar mass	M_g	4.0026×10^{-3}	kg/mol
Adiabatic expansion coefficient	γ	1.667	-
Specific heat at constant volume	c_v	3115.89	J/(kg·K)

As for the initial conditions, Table 4, this work assumes that the balloon is launch with null acceleration and null velocity, which translates in the following

$$\begin{cases} \ddot{z} = 0 \Rightarrow B + W + D = 0 \\ \dot{z} = 0 \Rightarrow D = 0 \end{cases} \Rightarrow B = -W \,. \tag{23}$$

Developing this equality allows to obtain the required initial mass of gas, for a set of parameters, as shown

$$\begin{aligned} &\rho_{atm} \cdot V_b \cdot g = m_T \cdot g \\ &\Leftrightarrow \rho_{atm} \cdot \frac{m_g R_g T_g}{M_g P_g} = m_{structure} + m_g + m_{ballast} \\ &\Leftrightarrow m_g = \frac{m_{structure} + m_{ballast}}{\frac{R_g T_g \rho_{atm}}{M_g P_g} - 1} \,. \end{aligned} \tag{24}$$

2.5.1. Validation

The balloon model was validated with and without the altitude controller. First, the balloon model was tested for ideal conditions, considering that it was

Table 4: Launch parameters.

Parameter	Symbol	Value	Units
Atmospheric temperature	T_{atm}	288.15	K
Atmospheric pressure	P_{atm}	101325	Pa
Atmospheric density	ρ_{atm}	1.225	kg/m^3
Gas temperature	T_g	288.15	K
Gas pressure	P_g	101500	Pa
Gas density	ρ_g	0.1696	kg/m^3
Mass of gas	m_g	0.3278	kg
Radius	R	0.7727	m
Volume	V_b	1.9329	m^3

not subject to wind disturbances nor to radiation (the only thermal effect considered was convection). As expected, the balloon was able to stay in equilibrium. Then, radiation and wind disturbances were added to the balloon system to better comprehend the behavior of the balloon when subject to real exterior conditions. This analysis showed that until 10000m the balloon falls slowly from the desired altitude, but after that there is a change in the radiation evolution and the balloon rises slowly from the defined altitude. The balloon system's behavior observed in real exterior conditions demonstrates that an altitude control should be implemented in order to be able to remain at a desired altitude level. Therefore, the balloon model was also validated with the altitude controller and it was demonstrated that the balloon system is able to maintain its altitude when subject to a real exterior environment, as seen in Figure 2.

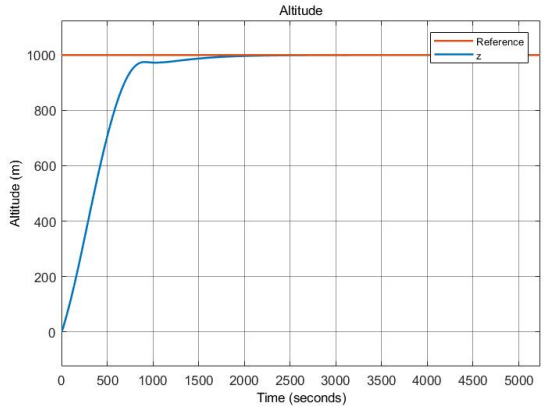

Figure 2: Evolution of the balloon's altitude, z.

3. Wind Analysis

The wind velocity components were collected from "ERA5 hourly data on pressure levels from 1940 to present" one of the many data sets that make up ERA5. The data is characterized by a regular latitude-longitude grid with a resolution of 0.25°$\times$ 0.25° and a global horizontal coverage, a vertical resolution of 37 pressure levels, from 1000hPa to 1hPa, and a hourly resolution from 1940 to the present. In order to download the desired data, the user must choose the variables of interest, which for this work are the "U-component of wind" (horizontal speed of air moving towards the east - longitudinal component, v_{wx}) and the "V-component of wind" (horizontal speed of air moving towards the north - latitudinal component, v_{wy}), the desired pressure levels (from the 37 available), the time resolution (year(s), month(s), day(s) and hour(s)), and the relevant geographical area (defined by latitude and longitude).

The pressure levels considered for the wind analysis are presented in Table 5 and the geographical area defined was $43°N - 36°N$ and $12°W - 4°W$. As mentioned before the horizontal resolution is 0.25°$\times$ 0.25°, which corresponds to 27.75km $\times$ 21.25km (latitude-longitude). Note that this correlation between degrees and kilometers is admissible for the geographical area selected but for different parts of the globe may differ.

Table 5: Pressure-altitude conversion.

P [hPa]	h [m]	P [hPa]	h [m]	P [hPa]	h [m]
1000	110.88	850	1457.30	600	4206.43
975	323.38	825	1700.13	500	5574.44
950	540.34	800	1948.99	400	7185.44
925	761.97	775	2204.23	300	9163.96
900	988.50	750	2466.23	200	11784.06
875	1220.19	700	3012.18		

3.1. Wind Statistical Analysis

The first wind analysis performed was an average variability analysis of the different meteorological trimesters, to acquire a global perception of the wind behavior. The meteorological trimesters are defined as follows: 1) **Winter:** December - January - February (DJF), 2) **Spring:** March - April - May (MAM), 3) **Summer:** June - July - August (JJA), and 4) **Autumn:** September - October - November (SON)

This analysis was made using NOAA Climate Plotting and Analysis Tools, which outputs a plot with the average velocity and direction of the wind, for the region, years, months and altitude level chosen. It is important to note that the meteorological angle defines 0° along the y-axis and increases clockwise, and that the meteorological wind direction corresponds to the direction **from** which the wind blows.

The results of this analysis lead to the conclusion that westerly winds are the most common in the selected area. Also, it is observed that the wind velocity is generally uniform across the entire region at each altitude level, with just a slight variance be-

tween the maximum and minimum values. Finally, it is noted that an increase in altitude corresponds to an increase in wind speed.

3.2. Wind Rose Analysis

In order to better understand the wind behavior and determine if it is feasible to use wind to guide the balloon to a desired location, a statistical analysis of the wind was made using wind roses. A wind rose is a graphical chart used by meteorologists that characterizes wind speed and direction at a certain location over a specified time period. This chart is presented in a circular format and shows the frequency of time that wind blows from particular directions.

Firstly, every month and trimester (DJF, MAM, JJA and SON) were analyzed through wind roses for every pressure level. Then, a daily and hourly analysis was also performed. Based on the data analyzed, it can be said that the wind direction behavior is more evident the more exact the study is, that is, the less average of time is considered.

The wind rose analysis leads to the conclusion that one can use the quarterly analysis to have a general idea of the wind behavior but should expect to have variability from month to month, day to day and even from hour to hour. Also, it is expected that by controlling the altitude of the balloon and having predictions of the wind one should be able to guide the balloon to different areas. The areas that the balloon will be able to reach will depend on the meteorological conditions of the selected day and launch hour. Although these factors can not be controlled, one can take advantage of daily wind predictions or even online trajectory predictors to infer which day or hour is preferable to launch the balloon according to the desired goal location.

4. Balloon Path Planning

Usually weather balloons drift freely in the prevailing wind at the operating altitude. The goal of this work is to optimize the balloon's trajectory, assuming that the balloon moves in the same direction as the wind and that the altitude control system is in place to allow the balloon to maintain its altitude.

Path optimization is achieved by selecting a trajectory that satisfies a specified set of criteria to reach a stated mission objective. Typically, the flight objective is to take the balloon from one point to another or to maintain the balloon around a certain area. Taking the flight objective into account, a pre-flight path planning must be developed to determine an optimal path so that not only the distance to the goal location is minimized but also the resources expenditure since the gas and ballast required to perform the altitude control are limited.

Based on the spacial and temporal wind information available, 3D wind grids (latitude, longitude and altitude) can be defined for different times, where each node has an associated wind vector (wind direction and velocity). The optimal path must be found within the wind vectors, moving from node to node, considering the balloon restrictions, namely the maximum altitude, velocity, and resources available.

The path planning algorithm must output a set of vertical actuation commands to the balloon simulator so that the balloon can be controlled in altitude and drift with the favorable wind currents. Since the balloon's movement is entirely dependent on the wind direction there will be times when the balloon will simply be unable to reach the desired location. In that case, other hours, days, and/or launch sites should be tested with the pre-flight path planning.

It should be noted that since the balloon is in the atmosphere, physical obstacles are not taken into account, and it is assumed that airspace is free to circulate in any zone.

4.1. A* Algorithm

After an overview of the optimization algorithms that are used for path planning, the A* algorithm was chosen for this work. The A* algorithm is an informed graph search algorithm which selects the nodes to be explored based on the best heuristic value. This characteristic directs the path search to the goal saving a significant amount of computation time. The cost function to be minimized is defined by

$$f(n) = g(n) + h(n)\,, \tag{25}$$

where $g(n)$ is the cost from the start node to node n and $h(n)$ is the heuristic function that estimates the cost from node n to the goal node.

4.2. Weighted A*

For more complex problems, with higher dimension graphs, the A* algorithm may take too long to find a feasible solution. In this case, a variation of A* can be used to find a solution faster, which explores less nodes. This alternative is called weighted A*, which multiples the heuristic by a weight (w) as shown

$$f(n) = g(n) + w \times h(n)\,. \tag{26}$$

4.3. Balloon Path Planning Solution

A mission objective must be defined so that the path planning optimization can be performed. For this work the following mission objectives were considered: 1) Take the balloon from one point (start) to another (goal), 2) Take the balloon to different pre-defined waypoints, and 3) Maintain the balloon around a certain area, whether it is a waypoint or the goal.

Since the balloon movement is restricted by the wind movement, reaching the goal may be challenging. Therefore the goal was defined in two dif-

ferent ways: either it is a point described by (latitude, longitude, altitude), or it is a vertical line described by (latitude, longitude), with no altitude restrictions.

Moreover, in order to apply the A* algorithm to the balloon path planning problem the cost function $f(n)$, the grid search space and the balloon's restrictions must be defined.

4.3.1. Configuration Space

In this work, the graph is defined by the wind grid, where each node has an associated wind direction and velocity (wind vector). The horizontal resolution is equivalent to a latitudinal resolution of 27.75km and a longitudinal resolution of 21.25km. As for the vertical resolution, the altitude levels were interpolated in order to have a regular resolution of 0.5km.

4.3.2. Constraints

Balloons have no maneuverability restrictions, meaning they can move in any direction, but because they have no lateral control their horizontal motion is entirely constrained by the movement of the wind. Therefore, even though theoretically during the process of node expansion the balloon could reach any of its neighboring nodes, Figure 3, in practice not all of them will be admissible because reaching them would require to go against the wind direction.

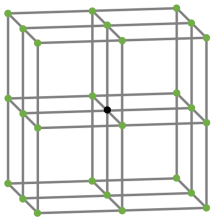

Figure 3: Representation of the balloon's neighboring nodes.

Only three out of the 26 neighboring nodes are admissible: one in the balloon's altitude level and the other two in the immediately upper and lower levels, which can be reached by controlling the balloon's altitude.

The admissible node at the balloon's altitude level is solely determined by the wind direction. Note that, the graph only has 8 possible directions in the 2D plane whereas the wind direction can take any value in the interval [0°, 360°]. Therefore, the wind direction must be approximated to one of the defined node directions. These approximations result in a deviation of the balloon's motion from the actual wind movement. The solution to minimize this error is to consider more possible directions in the grid. Hence, the case of 16 neighboring nodes was also explored.

For the upper and lower altitude levels, the admissible nodes are determined not only by the wind direction but also by the actuation and wind velocities. These velocities are important because while the balloon is moving vertically it is also being pushed horizontally. Therefore, the wind direction restricts the possible admissible nodes but the wind intensity determines which node will be the admissible one.

The process of node expansion for balloons is not fixed in time nor space and, therefore, for each node the admissible neighbor nodes must be determined based on the wind direction and intensity.

Another constraint is the limitation of resources, specifically gas and ballast which are required to perform the altitude control of the balloon. During the search process through the graph, the algorithm must take into account that there is a maximum amount of ballast to expend and that there must remain enough gas to perform a safe descent of the balloon.

Finally, the mission constraints are the waypoints/goal given to the path planner which the balloon must reach.

4.3.3. Cost Functions

Considering that in this work the objective is to plan a path that minimizes both the distance to the waypoint/goal node as well as the resources expenditure, the cost functions $h(n)$ and $g(n)$ were defined in the following way:

$h(n)$ is the Euclidean distance between node n and the waypoint/goal node, so that nodes closer to the goal are considered first or, in other words, so that minimum distance paths are prioritized in the search process. In the graph, the Euclidean distance is computed between the current node (x_c, y_c, z_c) and the final node (x_f, y_f, z_f), whether it is a waypoint or the goal node. Additionally, in order to account for the traveled kilometers, each component must be multiplied by the correspondent grid resolution (lat, lon or alt) as follows

$$h(n) = \sqrt{[(x_f - x_c) \times lat]^2 + [(y_f - y_c) \times lon]^2 + [(z_f - z_c) \times alt]^2}\,. \tag{27}$$

This is the expression used when the goal is a specific point, because it accounts for the altitude. However, if the goal is instead a vertical line with no altitude restriction the Euclidean distance is given by

$$h(n) = \sqrt{[(x_f - x_c) \times lat]^2 + [(y_f - y_c) \times lon]^2}\,, \tag{28}$$

$g(n)$ takes into account both the distance between the current node and its neighbor node n as well as the resources expended to reach the

neighbor. As a result, the nodes which require less resources to be reached are considered first and, therefore, paths that expend less resources are prioritized. The distance between the current node and its neighbor is computed with the Euclidean distance. The actuation cost, which is the cost associated to the resources expenditure, depends on the neighbor's altitude level. If the neighbor is at the same altitude level as the current node there is no actuation cost. On the other hand, if the neighbor is in the upper or lower altitude level there is an associated actuation cost because the altitude control system must be used to reached it. Moreover, this cost must be converted into a distance determined by the expended mass of gas and ballast because the costs that compose the function $g(n)$ must be in the same units in order to be summed. Therefore, the actuation cost is defined as

$$cost_{actuation} = \begin{bmatrix} m_{gas} & m_{ballast} \end{bmatrix} \begin{bmatrix} k_1 & 0 \\ 0 & k_2 \end{bmatrix} \begin{bmatrix} m_{gas} & m_{ballast} \end{bmatrix}^T, \quad (29)$$

where $k1$ and $k2$ are constants given in [km/kg] so that the $cost_{actuation}$ is expressed in kilometers.

Note that no cost was associated to the wind direction in each node, that is there is no penalization if the wind pushes the balloon in a direction other than the goal, because the balloon may have to move away from the goal in order to reach it.

5. Results and Discussion

The formulation of the balloon path planning solution is general, but in order to validate the algorithm the following parameters were defined:

- The balloon considered is the TA450 model;
- The altitude control strategy considered is the one presented in section 2, with helium and sand;
- The maximum gas (helium) mass is 0.328kg and the maximum ballast (sand) mass is 0.950kg. Also, the minimum gas mass necessary to hold the platform and perform a safe descend is 0.175kg;
- The actuation velocity (vertical velocity) of the balloon system is $v_{actuation} \simeq$ 0.6m/s;
- The resources expended each time the altitude control system is activated are $m_{gas} \simeq$ 0.006kg and $m_{ballast} \simeq$ 0.04kg;
- The constants required to compute the actuation cost are $k_1 = \frac{0.5}{0.006^2}$km/kg and $k_2 = \frac{0.5}{0.04^2}$km/kg, so that the $cost_{actuation}$ = 1;
- The launch time is defined as 15/09/2022 at 08:00 (if another launch time is considered, it will be identified in the results).

The algorithm works under the assumption that the balloon starts in an equilibrium position with null vertical velocity.

Furthermore, the optimal path determined by the algorithm must be processed in order to provide the balloon simulator with a continuous input. Also, due to the discrete nature of the algorithm, the paths will represent the worst case scenario in terms of resources expenditure because the algorithm assumes that the pre-defined mass of gas and ballast are always expended between each node (in different levels) regardless of whether the balloon is continuously ascending or descending.

5.1. Algorithm Validation

The different features of the balloon path planning solution were tested and validated:

Number of Possible Directions: The user can choose to either define 8 or 16 possible directions, in the 2D plane, for the balloon movement. In order to test which of the two options produces more accurate results, two trajectories were tested in the developed simulator. As expected, using 16 directions produces the best results because defining more directions in the graph allows the algorithm to follow the wind directions more precisely.

Type of Goal: In section 4.3 two types of goal were defined: 1) LLA or 2) LL. The performance of the algorithm was tested for the two types of goal, considering different scenarios. It was concluded that defining the goal only with (latitude, longitude) coordinates, without restricting the altitude, gives more flexibility to the algorithm and produces better results in terms of time, traveled distance and resources expenditure.

Weighted A*: The performance of the algorithm was analyzed using the following weights: 0 (Dijkstra's algorithm), 1 (A* algorithm), and 2 and 100 (greedy best-first search). This analysis showed that if there is an optimal path from start to goal, the algorithm will always find it regardless of the weight chosen. Furthermore, usually the weight is increased to make the algorithm converge faster, but in this work that is not justified as the algorithm gives an output in a matter of seconds, with w=1. Also, since the weight is associated to the heuristic cost function $h(n)$, increasing it might result in higher resources expenditure, which is not desired.

Actuation Cost: The actuation cost (equation 29) considered between each node is crucial because the resources required to perform the altitude control of the balloon are limited. Without the resources expenditure restriction, the algorithm finds the optimal path under the assumption that it

can spend whatever resources are available, within the maximum limits. As a result, it reaches the goal faster but expends more resources, which is not desired. On the other hand, defining the actuation cost as a positive number results in the same paths because regardless of the chosen value, the nodes that require altitude control to be reached will always have a higher cost that the nodes that do not.

Launch Time: The balloon's movement is restricted by the wind, so there will be occasions when the algorithm is unable to find an optimal path. Other times, although an optimal path is found, the user might want to test other alternatives in which the balloon does not overfly the ocean or the country borders, or the balloon takes shorter paths, etc. In order to choose the best launch time according to the desired objective, the user can input different launch times in the algorithm. The range of different trajectories obtained highlights the wind's variability, since a different trajectory was obtained for every scenario tested.

Launching Conditions: In order to highlight that the user can choose any location and height for the starting point, various scenarios were tested. This flexibility is important because according to the desired objective it might be favorable to launch the balloon from a location closer to the goal. On the other hand, due to airspace restrictions it might be necessary to fly the balloon at high altitudes.

Mission Objectives: In section 4.3, three mission objectives were defined, namely to take the balloon from one point to another, which has been used in every analyses discussed so far. Another mission objective was to maintain the balloon around a certain area. This objective proved to be more difficult to achieve because it requires specific wind conditions not only to get to the desired location but also to maintain the balloon there. Note that in order to consider that the balloon maintained its location, the algorithm must be able to return to the goal's LL location in successive iterations. The last mission objective proposed was to take the balloon to different pre-defined waypoints. This mission objective was tested for different scenarios, and the results were very satisfactory, as the algorithm was able to find optimal paths between the required waypoints across Portugal.

Azores Test Case: As mentioned in section 1, this work was developed in the scope of the SONDA project, which aims to monitor both the atmosphere and the ocean. Therefore, it is important to evaluate the performance of the algorithm over the ocean. Different scenarios were tested to infer if it would be possible to fly the balloon over the Azores islands. The region defined was $42°N - 34°N$ and $34°W - 22°W$. The algorithm was able to successfully find trajectories, but predefining waypoints proved to be challenging because the wind currents dragged the balloon away from the islands.

5.2. Planning and Control Validation

Having tested the different features and mission objectives of the path planning algorithm, it is also important to validate that the developed simulator is able to perform the planned trajectories. Therefore, the trajectory between Lisbon and Évora, with launch in 15/09/2022 at 08:00, was tested with the simulator. The results obtained were successful and are illustrated in Figure 4. Note that the simulator was not tested for the most complex cases because the realistic balloon model is heavy and the computational cost is too high for the computer used.

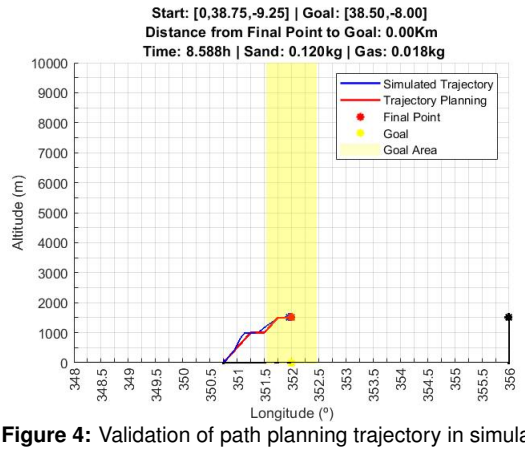

Figure 4: Validation of path planning trajectory in simulator.

5.3. Final Remarks

The results presented showed the advantages and relevance of the different features of the balloon path planning algorithm, and demonstrated successfully that it is possible to direct the balloon to different goals taking advantage of wind currents and using an altitude control strategy. Within the scenarios tested, the balloon was able to fly over the Azores islands and to reach the following regions of continental Portugal: North: Gerês, Lamego, Serra da Estrela; Center: Lousã, Pedrogão Grande, Serra de S.Mamede, Campo Maior; South: Évora, Beja, Odemira, Monchique.

Nevertheless, these analyses also demonstrated that since the balloon is subject to the wind movement, it is not always possible to reach the goal and, therefore, other launch times need to be tested. Other times, even if the goal is reached, different launch times might have to be considered in order to meet the required objectives. It is important to note that the results showed that frequently the balloon will have to move away from the goal in

order to reach it, resulting in extended flights.

Additionally, it is possible to conclude that the path planning algorithm was successful for all three mission objectives. However, maintaining the balloon around a certain area without lateral control proved to be more challenging and did not work on the majority of the tested days.

Finally, the validation with the simulator was successful which demonstrates that the path planning solution is feasible.

6. Conclusions

The main result of this work is a functioning balloon path planning algorithm. To achieve this result, firstly, a latex balloon was derived and a simulator was built for exterior conditions. Then, an extensive statistical analysis of the wind behavior in Portugal was performed to determine if it would be feasible to guide the balloon using wind currents. Finally, the balloon path planning solution was formulated and validated.

This working path planning algorithm combined with the realistic balloon simulator and the prototype developed by Bruno Cândido in the scope of the SONDA project can now be the first step to perform a controlled flight with a weather balloon outdoors.

References

[1] Paul Voss, Dan Holcomb, Carl Berkowitz, and Rahul Zaveri. Integrated system optimization of controlled meteorological (cmet) balloons. In *AIAA 5th ATIO and16th Lighter-Than-Air Sys Tech. and Balloon Systems Conferences*, page 7387, 2005.

[2] Öznur Kayhan, Özgün Yücel, and M Alaittin Hastaoğlu. Simulation and control of serviceable stratospheric balloons traversing a region via transport phenomena and pid. *Aerospace Science and Technology*, 53:232–240, 2016.

[3] Andrey Sushko, Aria Tedjarati, Joan Creus-Costa, Kai Marshland, Paige Brown, Davy Ragland, John Dean, Sasha Maldonado, and John M Pauly. Advancements in low-cost, long endurance, altitude controlled latex balloons (valbal). In *2018 IEEE Aerospace Conference*, pages 1–10. IEEE, 2018.

[4] Yago Henrique Melo Honda, Matheus Filippe Santos Alves, Ana Carolina Cabral Pimentel de Melo, Renato Alves Borges, Simone Battistini, Manuel Nascimento Dias Barcelos Júnior, and Chantal Cappelletti. Development of an altitude control system for the laicansat platform. In *2019 IEEE Aerospace Conference*, pages 1–8. IEEE, 2019.

[5] Sai Sudha Ramesh, Juanli Ma, Kian-Meng Lim, Heow Pueh Lee, and Boo Cheong Khoo. Numerical evaluation of station-keeping strategies for stratospheric balloons. *Aerospace Science and Technology*, 80:288–300, 2018.

[6] Yi Jiang, Mingyun Lv, Weiyu Zhu, Huafei Du, Lanchuan Zhang, and Jun Li. A method of 3-d region controlling for scientific balloon long-endurance flight in the real wind. *Aerospace Science and Technology*, 97:105618, 2020.

[7] KM Aaron, MK Heun, and KT Nock. A method for balloon trajectory control. *Advances in Space Research*, 30(5):1227–1232, 2002.

[8] Lars James Blackmore, Nanaz Fathpour, and Alberto Elfes. Graph-based path-planning for titan balloons. Technical report, 2010.

[9] Lars Blackmore, Yoshiaki Kuwata, Michael T Wolf, Christopher Assad, Nanaz Fathpour, Claire Newman, and Alberto Elfes. Global reachability and path planning for planetary exploration with montgolfiere balloons. In *2010 IEEE International Conference on Robotics and Automation*, pages 3581–3588. IEEE, 2010.

[10] Michael T Wolf, Lars Blackmore, Yoshiaki Kuwata, Nanaz Fathpour, Alberto Elfes, and Claire Newman. Probabilistic motion planning of balloons in strong, uncertain wind fields. In *2010 IEEE International Conference on Robotics and Automation*, pages 1123–1129. IEEE, 2010.

[11] Robert D Born and Mac Schwager. Riding an uncertain wind field: Receding horizon tree search planning with opportunistic sampling for an autonomous weather balloon. In *AIAA Scitech 2019 Forum*, page 0395, 2019.

[12] Ivano Musso, Andrea Cardillo, and Roberto Ibba. Genetic algorithms: trajectory optimization for stratospheric balloons. In *17th ESA Symposium on European Rocket and Balloon Programs and Related Research Sandefjord, Norway, ESA SP-590, Noordwijk, Holland*, pages 457–460, 2005.

[13] Ethan A Chaffee, Patrick Ellis, and Jan P Reguero-Inserni. Uncertainty quantification for high altitude balloon trajectory optimization. In *AIAA Aviation 2019 Forum*, page 3195, 2019.

[14] Bruno Cândido. Model identification and prototype development for altitude control of laboratorial balloon. Master's thesis, Instituto Superior Técnico, 2022.